
Online Decision MetaMorphFormer: A Casual Transformer-Based Reinforcement Learning Framework of Universal Embodied Intelligence

Luo Ji¹*, Runji Lin¹

¹ DAMO Academy, Alibaba Group
<https://rlodm.github.io/odm/>

Abstract

Interactive artificial intelligence in the motion control field is an interesting topic, especially when universal knowledge is adaptive to multiple tasks and universal environments. Despite there being increasing efforts in the field of Reinforcement Learning (RL) with the aid of transformers, most of them might be limited by the offline training pipeline, which prohibits exploration and generalization abilities. To address this limitation, we propose the framework of Online Decision MetaMorphFormer (ODM) which aims to achieve self-awareness, environment recognition, and action planning through a unified model architecture. Motivated by cognitive and behavioral psychology, an ODM agent is able to learn from others, recognize the world, and practice itself based on its own experience. ODM can also be applied to any arbitrary agent with a multi-joint body, located in different environments, and trained with different types of tasks using large-scale pre-trained datasets. Through the use of pre-trained datasets, ODM can quickly warm up and learn the necessary knowledge to perform the desired task, while the target environment continues to reinforce the universal policy. Extensive online experiments as well as few-shot and zero-shot environmental tests are used to verify ODM’s performance and generalization ability. The results of our study contribute to the study of general artificial intelligence in embodied and cognitive fields. Code, results, and video examples can be found on the website <https://rlodm.github.io/odm/>.

1 Introduction

Research of embodied intelligence focus on the learning of control policy given the agent with some morphology (joints, limbs, motion capabilities), while it has always been a topic whether the control policy should be more general or specific. As the improvement of large-scale data technology and cloud computing ability, the idea of artificial general intelligence (AGI) has received substantial interest Reed et al. [2022]. Accordingly, a natural motivation is to develop a universal control policy for different morphological agents and easy adaptive to different scenes. It is argued that such a smart agent could be able to identify its ‘active self’ by recognizing the egocentric, proprioceptive perception, react with exteroceptive observations and have the perception of world forward model Hoffmann and Pfeifer [2012]. However, there is seldom such machine learning framework by so far although some previous studies have similar attempts in one or several aspects.

Reinforcement Learning(RL) learns the policy interactively based on the environment feedback therefore could be viewed as a general solution for our embodied control problem. Conventional RL could solve the single-task problem in an online paradigm, but is relatively difficult to implement and slow in practice, and lack of generalization and adaptation ability. Offline RL facilitates the

*Corresponding author: jiluo.lj@alibaba-inc.com

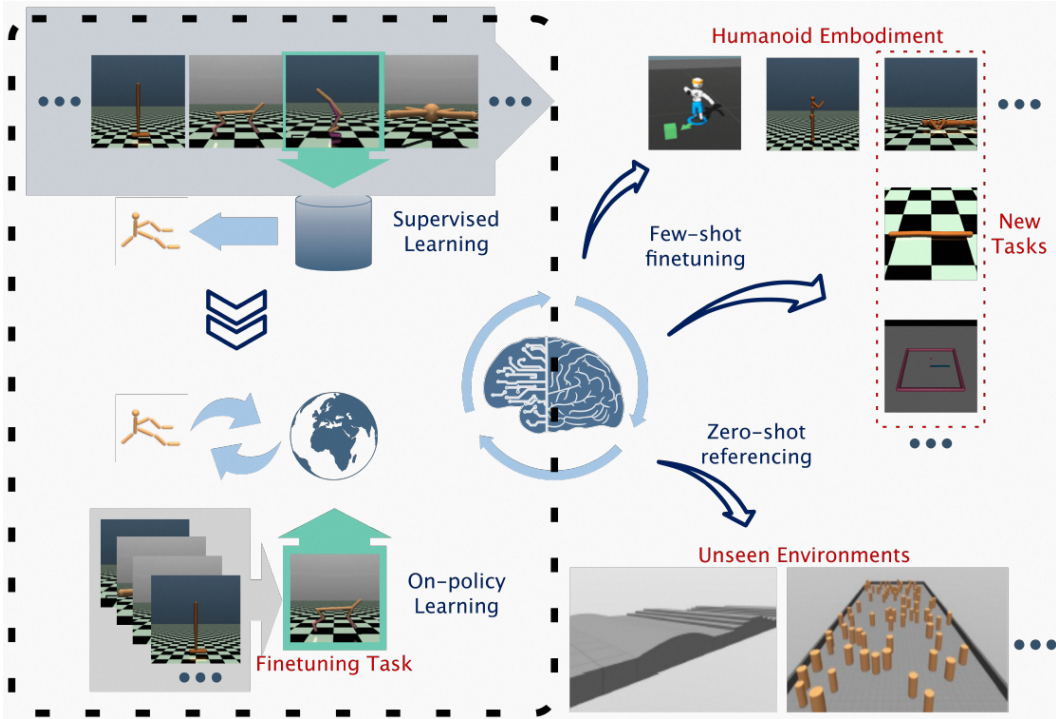


Figure 1: Application pipeline of ODM.

implementation but in cost of performance degradation. Inspired by recent progress of large model on language and vision fields, transformer-based RL Reed et al. [2022], Chen et al. [2021], Lee et al. [2022], Janner et al. [2021], Zheng et al. [2022], Xu et al. [2022] has been proposed by transforming RL trajectories as a large time sequence model and train it in the auto-regressive manner. However, most of these studies belong to offline RL which build a big sequence model problem and tries to learning from large-scale offline dataset. Such methods provide an effective approach to train a generalist agent for different tasks and environments, but usually have worse performance than classic RL, and fail to capture the morphology information. In contrast, MetaMorph Gupta et al. [2022] chooses to encode on agent’s body morphology and performs online learning, therefore has good performance but lack of time-dependency consideration.

In this work, we propose a framework called **Online Decision Metamorphmer (ODM)**, which aims to study the general knowledge of embodied control across different body shapes, environments and tasks, as indicated in Figure 1. The idea is motivated from the behavioral psychology in which agents improve their skill by actual practice, learning from others (teachers, peers or even someone with worse skills), or makes decision based on the perception of ‘the world model’ Ha and Schmidhuber [2018], Wu et al. [2022]. Our ODM is built upon a morphology-time transformer-based RL architecture and is compatible with both offline and online learning. The model contains the universal backbone and the task-specific modules. The task-specific modules capture the potential difference in agent body shapes, and the morphological difference is enhanced by a prompt based on characteristic of body shapes. We first pretrain this model with a curriculum learning, by learning demonstrations from the easiest to the hardest task, from the expert to beginners. The environment model prediction is added as an auxiliary loss. The same architecture can then be finetuned online given a specific task. During the test, we are able to test ODM with all training environments, transfer the policy to different body shapes, adaptive to unseen environments and accommodate with new types of tasks (e.g. from locomotion to reaching, target capturing or escaping from obstacles.).

Main contributions of this paper include:

- We design a unified model architecture to encode time and morphology dependency simultaneously which bridges sequential decision making with embodiment intelligence.

- We propose a training paradigm which mimic the process of natural intelligence emerging, including learning from others, boost with practices, and recognize the world.
- We train and test our framework with agent in eight different body shapes, different environment terrain and different task types. These comprehensive analysis verifies the general knowledge of motion control learned by us.

The rest of the paper is organized as follows. The connection with previous works is first discussed in Related Work. We then introduce the preliminaries and the problem formulation. Our methodology and corresponding algorithms are stated in the Method. We summarize our results and compare with previous baselines in Experiment. We discuss the shortcomings and potential improvements in Discussion and finally concludes the paper.

2 Related Work

Classic RL: Among conventional RL methods, on-policy RL such as Proximal Policy Optimization (PPO) Schulman et al. [2017] is able to learn the policy and therefore has a good adaptive ability to environment, but is slow to convergence and might have large trajectory variations. Off-policy RL such as DQN Mnih et al. [2015] improves the sampling efficiency but still requires the data buffer updated dynamically. In contrast, offline RL Fujimoto et al. [2019], Kumar et al. [2020], Kostrikov et al. [2021] can solve the problem similar to supervised learning, but might have degraded performance because of the distribution shift between offline dataset and online environment. In our work, we aim to reach state-of-the-art performance for different embodied control tasks, therefore a model architecture compatible with on-policy RL is proposed.

Transformer-based RL: Among these efforts, Decision Transformer (DT) Chen et al. [2021] and Multi-game Decision Transformer Lee et al. [2022] embodied the continuous state and action directly and use a GPT-like casual transformer to solve the policy offline. Their action decision is conditioned on Return-to-Go (RTG), either arbitrarily set or estimated by the model, since RTG is unknown during inference. Instead, Trajectory Transformer (TT) Janner et al. [2021] discards RTG in the sequential modeling to avoid that approximation. PromptDT Xu et al. [2022] adds the task difference consideration into the model by using demonstrated trajectory as prompts. ODT Zheng et al. [2022] first attempts to solve transformer-based RL in an online manner but mainly focus on supervised on actions instead of maximizing rewards. In our work, we propose a similar model architecture that is able to conduct both offline learning and on-policy, actor-critic learning. Online learning employs PPO as the detailed policy update tool with the objective as reward maximization.

Morphology-based RL: There are some other studies that focus on the agent’s morphology information, including GNN-based RL which models agent joints as a kinematics tree graph Huang et al. [2020], Amorpheus Kurin et al. [2021] which encodes a policy modular for each body joint, and MetaMorph Gupta et al. [2022] which intuitively use a transformer to encode the body morphology as a sequence of joint properties and train it by PPO. In our work, we have the morphology-aware encoder which is similar with MetaMorph and has the same PPO update rule. However, compared with MetaMorph, we encode the morphology on not only the state but also historical actions, and consider the historical contextual consideration.

3 Preliminaries and Problem Setup

3.1 Reinforcement Learning

We formulate a typical sequential decision-making problem, in which on each time step t , an embodied agent conceives a state $s_t \in \mathcal{R}^{n_s}$, performs an action $a_t \in \mathcal{R}^{n_a}$, and receives a scalar reward $r_t \in \mathcal{R}^1$. Given the current state, the agent generates an action from its policy $\pi(a_t|s_t)$ and push the environment stage forward. This interactive process yields the following episode sequence:

$$\tau_{0:T} = \{s_0, a_0, r_0, s_1, a_1, r_1, \dots, s_T, a_T, r_T\} \quad (1)$$

in which T means the episode ends or reaching the maximum time length.

Reinforcement Learning (RL) is usually employed to solve such a problem by finding π such that $\max_{\pi} \mathbb{E}_{\tau \sim \pi}(R)$ in which the episode return defined as

$$R := \sum_{t=0}^T \gamma^t r_t \quad (2)$$

with $\gamma \in [0, 1)$ as the discounted factor.

Table 1: Comparison of Conventional RL and Our Notations

	State	Action
Conventional RL	$s \in \mathcal{R}^{n_s}$	$a \in \mathcal{R}^{n_a}$
Our approach	$o^{pro}, \mathcal{M}_s^{pro} \in \mathbb{R}^{K \times n}, o^{ext} \in \mathbb{R}^x$ $s = [o^{pro}, o^{ext}]$	$a, \mathcal{M}_a \in \mathbb{R}^{K \times m}$
Connections	$n_s = K * n - \sum \mathcal{M}_s + x$	$n_a = K * m - \sum \mathcal{M}_a$

3.2 Proximal Policy Optimization

The classical Proximal Policy Optimization (PPO) methodology Schulman et al. [2017] inherits from the famous actor-critic framework in which a critic estimates the state value function $V(s)$, while an actor determines the policy. The critic loss is calculated from Bellman function by bootstrapping the state value function

$$L^{\text{Critic}} = \mathbb{E}_{s \sim d^{\pi}} [r_t + \gamma(V_{\theta_{\text{old}}}(s_{t+1}) - V_{\theta}(s_t))^2]$$

On the other hand, generalized advantage estimation (GAE) Schulman et al. [2016] is employed to help calculate the action advantage A_t by traversing the episode backward

$$\begin{aligned} \hat{A}_t &= \delta_t + (\gamma\lambda)\delta_{t+1} + \dots + (\gamma\lambda)^{T-t+1}\delta_{T-1} \\ \delta_t &= r_t + \gamma V(s_{t+1}) - V(s_t) \end{aligned} \quad (3)$$

the actor is then learned by maximizing the surrogate objective of A_t according to the policy-gradient theorem

$$L^{\text{Actor}} = \text{CLIP}(\mathbb{E}_t \frac{\pi_{\theta_{\text{old}}}(a_t|s_t)}{\pi_{\theta}(a_t|s_t)} \hat{A}_t - \beta \text{KL}[\pi_{\theta_{\text{old}}}(\cdot|s_t), \pi_{\theta}(\cdot|s_t)])$$

in which the CLIP function means clipping the object by $[1 - \epsilon, 1 + \epsilon]\hat{A}_t$, and KL denotes the famous K-L divergence. A PPO policy update is then conducted by minimizing the objective upon each iteration:

$$L^{\text{PPO}} = -\eta_A L^{\text{Actor}} + \eta_C L^{\text{Critic}} \quad (4)$$

3.3 Problem Setup

Here we redefine the aforementioned conventional RL notations in a more ‘embodied style’, although still generalized enough for any arbitrary agent with a multi-joint body. Inspired by the idea of Gupta et al. [2022], we differentiate the observation into the agent’s proprioceptive observations, the agent’s embodied joint-wise self-perception (e.g. angular, angular velocity of each joint), as well as the exteroceptive observation, which is the agent’s global sensory (e.g. position, velocity). Given a K -joint agent, we denote the proprioceptive observation by $o^{pro} \in \mathbb{R}^{K \times n}$ in which each joint is embedded with n dimension observations. The exteroceptive observation is x -dimensional which results in $o^{ext} \in \mathbb{R}^x$ and $s := [o^{pro}, o^{ext}]$.

Stepping forward from Gupta et al. [2022], we also define the action in the joint-dependent way; that is, assuming each joint has m degree of freedom (DoF) of movements (e.g. torque), the action is reshaped as $a \in \mathbb{R}^{K \times m}$. To allow the room of different agent body shapes, we introduce binary masks which have the same shapes of o^{pro} and a and zero-pad the impossible observations or actions (e.g. DoF of a humanoid’s forearm should be smaller than its upper-arm due to their physical connection). Table 1 visualizes the comparison between the conventional RL notations and our embodied version notations.

3.4 Attention-based Encoding

Given a stacked time sequence vector $x \in \mathbb{R}^{T \times e}$ with T as the time length and e as the embedding dimension, an time sequence encoder can be expressed as

$$\text{Enc}_T(x) = \text{Attention}(Q=x, K=x, V=x) \in \mathbb{R}^{T \times e} \quad (5)$$

according to the self-attention mechanism Vaswani et al. [2017] with Q, K, V denoting query, key and value. Analogously, given a stacked joint sequence vector $p \in \mathbb{R}^{K \times e}$ with K as the number of joints, a morphology-aware encoder instead learns the latent representation on this joint sequence

$$\text{Enc}_M(p) = \text{Attention}(Q=p, K=p, V=p) \in \mathbb{R}^{K \times e} \quad (6)$$

By pre-tokenizing either o^{pro} or a into p , within the latent space with dimension e , their 'pose' latent variables can be encoded by Enc_M . For each form of encoder, timestep or joint position info is encoded by lookup embedding then adding to encoded vector. More details can be referred to the MetaMorph paper Gupta et al. [2022].

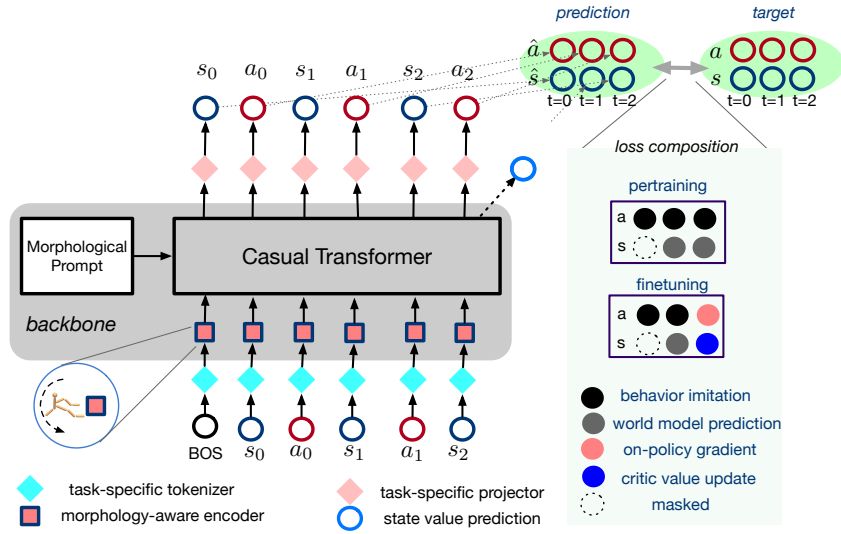


Figure 2: Model Structure of ODM and Corresponding Training Paradigm.

4 Methodology

We have developed a specialized transformer model architecture that includes a morphology-dependent encoder and decoder to model the trajectory sequence over time. A two-stage training paradigm is proposed that involves general pre-training on diverse offline data followed by task-specific fine-tuning training.

4.1 Model Architecture

Our ODM model structure contains a unified backbone and task-specific modules. Within this paper's context, the task might be related to a different agent (potentially different body types), environment, and reward mechanisms. Since the original system variables might have different dimensions, task-specific modules map them into a uniform-dimensional latent space (e in Eq. 6) and reverse operations. The backbone has a two-directional, morphology-time transformer structure, including morphology-aware encoders and a casual transformer. Architecture details are specified in Fig 2.

Tokenizer At each time t , observations and actions are first embedded into the latent space

$$\begin{aligned} o_t^e &= \text{Embed}_o(o_t^{pro}) \in \mathbb{R}^{K,e} \\ x_t^e &= \text{Embed}_x(o_t^{ext}) \in \mathbb{R}^e \\ a_t^e &= \text{Embed}_a(a_t) \in \mathbb{R}^{K,e} \end{aligned} \quad (7)$$

Morphology-aware Encoder Corresponding pose embedding vectors are obtained by traversing the agent’s kinematic tree and encoding the morphology by Eq. 6:

$$\begin{aligned} o_t^p &= \text{Enc}_M(o_t^e) \\ s_t^p &= \text{MLP}_s([s_t^p, x_t^e]) \in \mathbb{R}^e \\ a_t^p &= \text{Enc}_M(a_t^e) \end{aligned} \quad (8)$$

Casual Transformer To capture the morphology difference, we apply the prompt technique as in Xu et al. [2022], but embedding the morphology specifications instead of imitations

$$\text{Prompt} = \text{Embed}(K, n, m, x) \quad (9)$$

The casual transformer then translates the prompt and the input sequence into the output sequence

$$\text{output} = \text{Enc}_T(\text{Prompt}, \text{input}) \quad (10)$$

$$\text{input} := \{\text{BOS}, s_0^p, a_0^p, s_1^p, \dots, \dots, a_{t-1}^p, s_t^p\} \quad (11)$$

$$\text{output} := \{\hat{s}_0^p, \hat{a}_0^p, \hat{s}_1^p, \hat{a}_2^p, \dots, \dots, \hat{s}_t^p, \hat{a}_t^p\} \quad (12)$$

with a forward casual time mask. Detailed structure is inherited from GPT2, a decoder-only structure as in Chen et al. [2021], Janner et al. [2021], Zheng et al. [2022]. For practical consideration, input and output sequences are truncated by a window length T_w , with a padding time mask for episodes shorter than T_w . The timestep embedding is also considered and concatenated into the latent variable.

To emphasize the instant impact, we further conduct multi-head attention by querying the target variable and marking the input variable as key and value:

$$\begin{aligned} \hat{a}_t^p &\leftarrow \hat{a}_t^p + \text{Attention}(\text{Q}=\hat{a}_t^p, \text{K}=s_t^p, \text{V}=s_t^p) \\ \hat{s}_t^p &\leftarrow \hat{s}_t^p + \text{Attention}(\text{Q}=\hat{s}_t^p, \text{K}=a_{t-1}^p, \text{V}=a_{t-1}^p) \end{aligned}$$

Projector The task-specific projectors map latent outputs back to the original spaces:

$$\hat{a}_t = \text{Proj}_a(\hat{a}_t^p), \quad \hat{s}_t = \text{Proj}_s(\hat{s}_t^p), \quad \hat{V}_t = \text{Proj}_V(\hat{s}_t^p) \quad (13)$$

$\text{Embed}_o, \text{Embed}_x, \text{Embed}_a, \text{Embed}_s, \text{Proj}_a, \text{Proj}_s, \text{Proj}_V$ are all modeled as MLPs with LayerNorm and Relu between layers. More configuration details are on the website.

4.2 Training paradigm

ODM has a two-phase training paradigm including pretraining and finetuning, as in Algorithm 1.

Pretraining To mimic the learning process of the human infant, we design a curriculum-based learning mechanism in which the training dataset transverses from the easiest to the most complicated one. During each epoch, the current dataset is trained in an auto-regressive manner with two loss terms:

$$\begin{aligned} L^{\text{imitation}} &= \text{MSE}(\hat{a}_t, a_t^p), \quad L^{\text{prediction}} = \text{MSE}(\hat{s}_t, s_t^p) \\ L^{\text{pretrain}} &= \eta_i L^{\text{imitation}} + \eta_p L^{\text{prediction}} \end{aligned} \quad (14)$$

where MSE denotes the mean-square-error. $L^{\text{imitation}}$ corresponds to the imitation of action from demonstrations, while $L^{\text{prediction}}$ encourages the agent to reconstruct observations in the existence of casual mask².

Finetuning one extra predict head is activated to predict the state value \hat{V}_t ; this head as long as the very last prediction head of \hat{a}_t are employed as outputs of actor and critic:

$$\hat{V}_t \rightarrow V(s_t), \quad \hat{a}_t \rightarrow \pi(s_t) \quad (15)$$

Actor and critic can then be trained by PPO. Keeping some extent of L^{pretrain} as auxiliary loss, this finetuning becomes a self-supervised (and model-based, in the aspect of state-action jointly learning) RL

$$L^{\text{finetune}} = \eta_1 L^{\text{PPO}} + \eta_2 L^{\text{pretrain}} \quad (16)$$

² $L^{\text{prediction}}(t = 0)$ is masked out since it is meaningless to predict the very first state which is randomly initiated.

Algorithm 1 ODM

```
1: Initialize  $\theta$ 
2: Pretraining:
3:   set num of epoch = 0
4:   SWITCH between 6 body shapes :
5:     activate the current env-specific module
6:     freeze grads of other env-specific modules
7:     REPEAT learning from varied pioneers
8:       training on  $L^{\text{pretrain}}$  of mini-batch
9:     increment num of epoch
10: Finetuning:
11:   load the model in the target environment
12:   REPEAT iterations:
13:     for each actor do
14:       run current policy  $\pi$  for  $T$  steps
15:       compute advantages  $\hat{A}_0, \dots, \hat{A}_T$ 
16:     end for
17:     update  $\theta$  with  $L^{\text{finetune}}$  on a mini-batch
18:     stop when converges
```

5 Experiments

This section highlights our experiment setup and results. Further details (such as the videos) can be found on our website.

5.1 Configurations

Table 2 introduces the configuration details of our experiments, including the environments, agents, baselines, and demonstration pioneers. For further details of hyper-parameters, please refer to Table 8 in the appendix.

Table 2: Environment morphology details

Environment	K	n	m	x	m_s	m_a	n_s	n_a
swimmer	2	2	1	4			8	2
reacher	2	3	1	5			11	2
hopper	3	2	1	5			11	3
halfCheetah	6	2	1	5			17	6
walker2D	6	2	1	5			17	3
ant	8	2	1	95			111	8
humanoid	9	6	3	342	20	10	376	17
walker	16	15	4	18	45	25	243	39
unimal	12	52	2	1410	*	*	624	24

*: varied from each agent morphology.

5.1.1 Environments & Agents

We practice with enormous agents, environments and tasks, to validate the general knowledge studied by ODM. These scenes include:

Body shape: including swimmer (3-joints, no foot), reacher (1-joint and one-side fixed), hopper (1 foot), halfcheetah (2-foot), walker2d (2-foot), ant (4-foot), and humanoid on the gym-mujoco platform³; walker (the agent called ragdoll has a realistic humanoid body)⁴ on the unity platform Juliani et al. [2018]; and finally unimal, a mujoco-based environment which contain 100 different morphological agents Gupta et al. [2021].

³www.gymnasium.dev/environments/mujoco/

⁴github.com/Unity-Technologies/ml-agents

Table 3: Pretraining dataset details

Environment	Source	sampling agent	# samples	# episodes	ave ep return	ave ep length
hopper	D4RL	expert	999,494	1,027	3511.36±328.59	973.22±97.84
	D4RL	medium-expert	1,999,400	3,213	2089.88±1039.96	622.28±263.22
	D4RL	medium	999,906	2,186	1422.06±378.95	457.41±110.88
	D4RL	medium-replay	402,000	2,041	467.30±511.03	196.96±195.15
	D4RL	random	999,996	45,239	18.40±17.45	22.10±11.99
halfCheetah	D4RL	expert	1,000,000	1,000	10656.43±441.68	1000.00±0.0
	D4RL	medium-expert	2,000,000	2,000	7713.38±2970.24	1000.00±0.0
	D4RL	medium	1,000,000	1,000	4770.33±355.75	1000.00±0.0
	D4RL	medium-replay	202,000	202	3093.29±1680.69	1000.00±0.0
	D4RL	random	1,000,000	1,000	-288.80±80.43	1000.00±0.0
walker2D	D4RL	expert	999,214	1,000	4920.51±136.39	999.21±24.84
	D4RL	medium-expert	1,999,209	2,190	3796.57±1312.28	912.88±194.62
	D4RL	medium	999,995	1,190	2852.09±1095.44	840.33±240.13
	D4RL	medium-replay	302,000	1,093	682.70±895.96	276.30±263.13
	D4RL	random	999,997	48,907	1.87±5.81	20.45±8.46
ant	D4RL	expert	999,877	1,034	4620.73±1409.06	967.00±140.87
	D4RL	medium-expert	1,999,823	2,236	3776.93±1509.93	894.38±243.20
	D4RL	medium	999,946	1,202	3051.06±1180.59	831.90±290.71
	D4RL	medium-replay	302,000	485	976.05±1005.71	622.68±140.87
	D4RL	random	999,930	5,821	-58.07±97.76	171.78±281.25
walker	self	ppo	1,001,861	7,928	262.74±281.18	126.37±119.17
unimal	self	metamorph	1,638,400	3,710	2.52±5.21	410.44±410.57

Environment: flat terrain (FT), variable terrain (VT) or escaping from obstacles.

Task: pure locomotion, standing-up (humanoid), or target reaching (reacher, walker).

Table 2 exhibit all environments and their the morphological dimensions. Environments are from platforms including gym-mujoco, unimal and unity.

5.1.2 Baselines

We compare ODM with four baselines, each representing a different learning paradigm:

Metamorph: a morphological encoding-based online learning method to learn a universal control policy Gupta et al. [2022].

DT: As a state-of-the-art offline learning baseline, we implement the decision transformer with the expert action inference as in Lee et al. [2022] and deal with continuous space as in Chen et al. [2021]. We name it DT in the following sections for abbreviation.

PPO: The classical on-policy RL algorithm Schulman et al. [2017]. Code is cloned from stable-baseline3 in which PPO is in the actor-critic style.

Random: The random control policy by sampling each action from uniform distribution from its bounds. This indicates the performance without any prior knowledge especially for the zero-shot case.

5.1.3 Demonstrating pioneers

For purpose of pretraining, we collect offline data samples of hopper, halfcheetah, walker2d and ant from D4RL Fu et al. [2020], as sources of pioneer demonstrations. For these environments, D4RL provides datasets sampled from agents of different skill levels, which corresponds to different learning pioneers in our framework, including *expert*, *medium-expert*, *medium*, *medium-replay* and *random*. We also train some baseline expert agents and use them to sample offline datasets on walker and unimal. This dataset contains more than 25 million data samples, with detailed statistics shown on our website. Within each curriculum, we also rotate demonstrations from the above pioneers for training, as indicated in Algorithm 1.

5.2 Pretraining

Model is trained with datasets of hopper, halfcheetah, walker2d, ant, walker and unimal, from the easiest to the most complex. Table 3 shows statistics of all dataset used in the pretraining phase. Pretraining is computed distributed on 4 workers, each with 8 gpu, 4000 cpu and 400M memory. For both pretraining and finetuning, the ADAM optimizer is applied with the decay weight of 0.01.

Figure 3 shows the loss plot. One can observe that the training loss successfully converges within each curriculum course; although its absolute value occasionally jumps to different levels because of the environment (and the teacher) switching. Validation set accuracy is also improved with walker and unimal as exhibition examples in Figure 3.

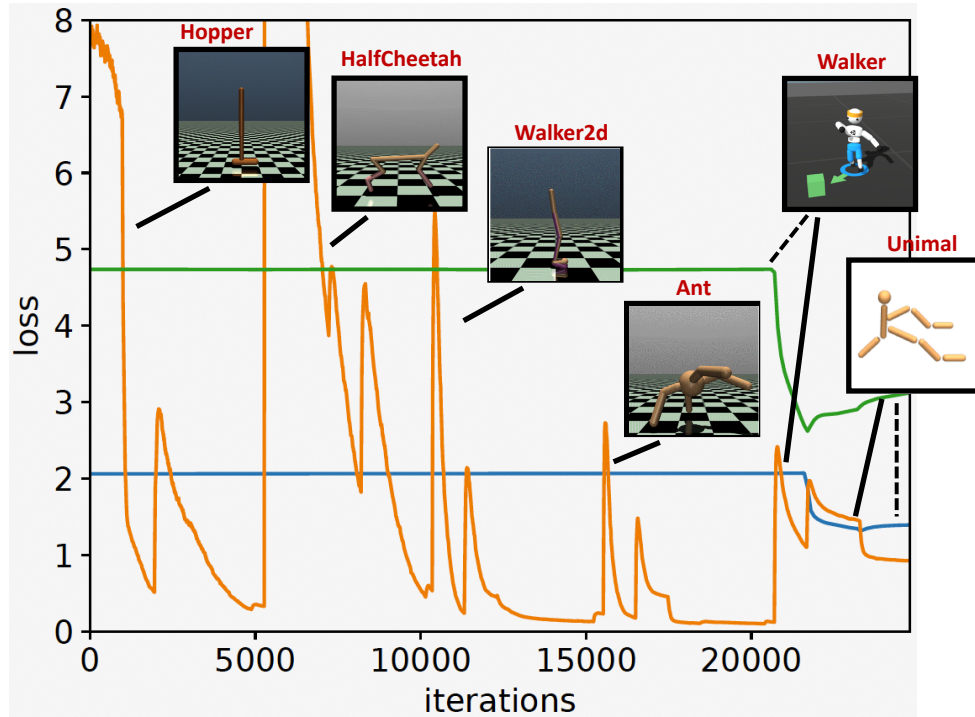


Figure 3: Time plot of pretraining performance. Orange: training loss. Green: validation MSE of walker; Blue: validation MSE of unimal.

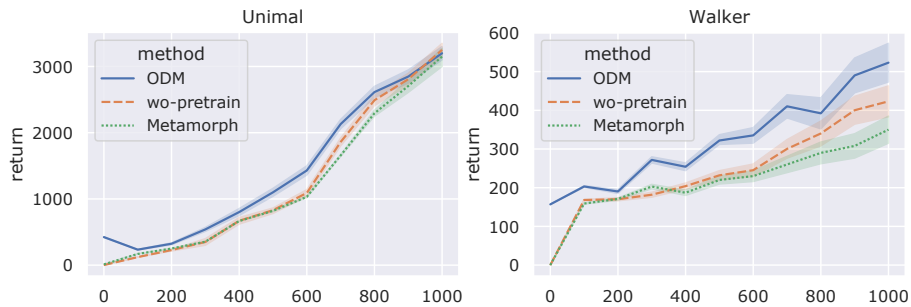


Figure 4: Comparison of averaged episode returns as functions of iterations during online experiments. Left: unimal. Right: walker. Curves are smoothed and values are rescaled for better visualization purposes.

Table 4: Averaged Episodic Performance in online locomotion environments.

Metric	Env.	ODM	MetaMorph	DT	PPO	Random
return	walker*	331.88 ±280.96	303.933±279.16	252.74±281.18	265.23±275.32	0.55±0.83
	unimal	3197.22±228.04	3251.68 ±192.61	-0.09±3.75	2507.32±260.71	-3.54±4.97
length	walker*	133.29 ±35.88	128.42±33.52	126.37±33.73	128.56±34.06	10.34±1.55
	unimal	917.85±40.84	931.92 ±33.21	347.36±66.47	884.39±50.34	321.98±71.49

*: Metrics of walker have substantial deviations since walker has forward process noise implemented.

5.3 Online Experiments

To make online learning faster, we use 32 independent agents to sample the trajectory in parallel, with 1000 as the maximum episode steps. The experiment continues more than 1500 iterations after the performance converges. Figure 4 provides a quick snapshot of online performances. Compared with ODM without pretraining, returns of ODM are higher at the very beginning, indicating knowledge from pretraining is helpful. As online learning continues, the performance degrades slightly until finally grows up again, and converges faster than the other two methods, although the entire training time (pretraining plus finetuning) is longer.

During online testing, 100 independent episodes are sampled and analyzed to evaluate the agent’s performance. The average episode return and episode length are recorded in Table 4. One can observe that our ODM outperforms MetaMorph (in walker) or is similar to MetaMorph (in unimal). Note there are large performance deviations in walker since this environment has substantial process noise implemented to challenge the learning. It is also worth noting that DT does not work for unimal, indicating the limitation of the pure offline method with changing agent body shapes.

5.4 Few-shot Experiments

We examine the transfer ability of policy by providing several few-shot experiments. Pretrained ODM is loaded in several unseen tasks, which are listed in Table 5. As a few-shot test, online training only lasts for 500 steps before testing. ODM obtains the best performance except for humanoid on flat terrain, indicating ODM has better adaptation ability than MetaMorph.

Table 5: Performance in few-shot experiments.

Metric	Env.	Task	ODM	MetaMorph	PPO	Random
return	unimal	obstacle	1611.86 ±179.38	1288.15±127.48	932.34±79.45	-2.08±4.85
	unimal	VT	580.10 ±41.23	499.58±35.21	310.02±22.93	-4.87±8.19
	swimmer	FT	145.58 ±16.97	143.01±11.31	142.36±13.31	0.14±2.00
	reacher	target reaching	-32.97 ±5.18	-33.28±4.58	-34.28±4.56	-42.96±0.15
	humanoid	FT	359.90±54.84	360.87±51.28	360.70 ±50.28	108.13±0.83
	humanoid	standup	76388.12 ±906.01	75750.41±897.01	75033.74±895.20	38921.67±451.25
length	unimal	obstacle	827.85 ±53.25	771.38±50.18	619.82±68.35	322.05±65.81
	unimal	VT	780.23 ±89.02	764.48±77.73	524.10±59.92	542.70±88.76
	swimmer	FT	1000	1000	1000	1000
	reacher	reaching	50*	50*	50*	50*
	humanoid	FT	68.10 ±3.15	66.85±3.94	67.59±2.34	22.15±0.17
	humanoid	standup	1000	1000	1000	1000

*: The official reacher environment has a maximum episode length limit of 50.

5.5 Zero-shot Experiments

Zero-shot experiments can be conducted by inferencing the model directly without any online finetuning. The unimal environment allows such experiment in which the flat terrain (FT) can be replaced by variable terrain (VT) or obstacles. Results are shown in Table 6. It can be observed that ODM reaches state-of-the-art performance for zero-shot tests, indicating that ODM has strong generalization ability by capturing general high-level knowledge from pretraining, even without any prior experience.

Table 6: Performance in zero-shot experiments.

Metric	Env.	Task	ODM	MetaMorph	DT	Random
return	unimal	obstacle	1271.70 ±182.34	1137.52±178.60	-0.55±3.06	-2.08±4.85
	unimal	VT	521.08 ±34.48	480.29±23.21	8.22±6.70	-4.87±8.19
length	unimal	obstacle	750.99 ±86.23	736.90±75.16	228.20±55.74	322.05±65.81
	unimal	VT	698.80 ±69.49	664.63±72.25	585.13±83.54	542.70±88.76

Table 7: Performance in ablation studies on unimal and walker.

Metric	Env.	Task	ODM	wo pretrain	wo finetune	wo curriculum	wo prompt
return	unimal	FT	3197.22 ±228.04	2331.36±131.24	463.12±84.55	434.44±73.43	453.41±80.13
	unimal	obstacle	1611.86 ±179.38	592.96±89.92	80.65±34.91	78.34±32.52	75.23±32.21
	unimal	VT	580.10 ±41.23	404.68±122.46	70.23±31.31	69.34±30.34	70.01±32.05
	walker	FT	331.88 ±280.96	313.49±260.35	112.64±72.23	109.34±68.19	111.82±69.76
length	unimal	FT	917.85 ±40.84	845.78±79.55	436.46±70.0	433.24±70.0	436.46±70.0
	unimal	obstacle	827.85 ±53.25	554.89±59.02	232.12±37.02	239.12±29.13	230.78±35.98
	unimal	VT	780.23 ±89.02	526.22±34.61	209.75±35.41	205.51±33.34	204.14±30.61
	walker	FT	133.29 ±35.88	105.29±40.13	84.32±34.17	80.41±33.41	82.14±35.43

5.6 Ablation Studies

To verify the effectiveness of each model component, we conduct the ablation tests for ODM with only the online finetuning phase (wo pretrain) and with only pretraining (wo finetune); within the pretraining scope, we further examine ODM without the curriculum mechanism (wo curriculum) and morphology prompt (wo prompt). The DT method could be viewed as the ablation of both $L^{\text{prediction}}$ and L^{PPO} , so we do not list the ablation results of these two loss terms. We conduct the ablation study on unimal (all 3 tasks) as well as walker, with results shown in Table 7. Results show that ODM is still the best on all these tasks, which indicating both learning from others’ imitation and self-experiences are necessary for intelligence agents.

5.7 Typical Visualizations

Generalist learning not only aims to improve the mathematical metrics, but also the motion reasonability from human’s viewpoint. It is difficult for traditional RL to work on this issue which only solve the mathematical optimization problem. By jointly learning other agent’s imitation and bridge with the agent’s self-experiences, we assume ODM could obtain more universal intelligence about body control by solving many different types of problems. Here we provide some quick visualizations about generated motions of ODM, comparing with the original versions ⁵.

By examining the agent motion’s rationality and smoothness, we first visualize the motions of trained models in the walker environment. Since the walker agent has a humanoid body (the ‘ragdoll’), the reader could easily evaluate the motion reasonability based on real-life experiences. Figure 5 exhibits key frames of videos at the same time points. In this experiment, we force the agent to start from exactly the same state and remove the process noise. By comparing ODM (the bottom line) with PPO (the upper line), one can see the ODM behaves more like a human while PPO keeps swaying forward and backward and side to side, with unnatural movements such as lowering shoulders and twisting waist.

We compare the motion agility by visualizing the unimal environment, in which the agent is encouraged to walk toward arbitrary direction. Figure 6 compares ODM with Metamorph. Metamorph wastes most of the time shaking feet, fluid, and gliding, therefore ODM walks a longer distance than Metamorph, within the same time interval ⁶.

6 Discussion

Our work can be viewed as an early attempt of an embodied intelligence generalist accommodated for varied body shapes, tasks, and environments. One shortcoming of the current approach is that ODM still has task-specific modules (tokenizers and projectors) for varied body shapes. By using

⁵Full version of videos can be found on the website <https://rlodm.github.io/odm/>

⁶Figure grids could help the reader to recognize the comparison although the video is more obvious.

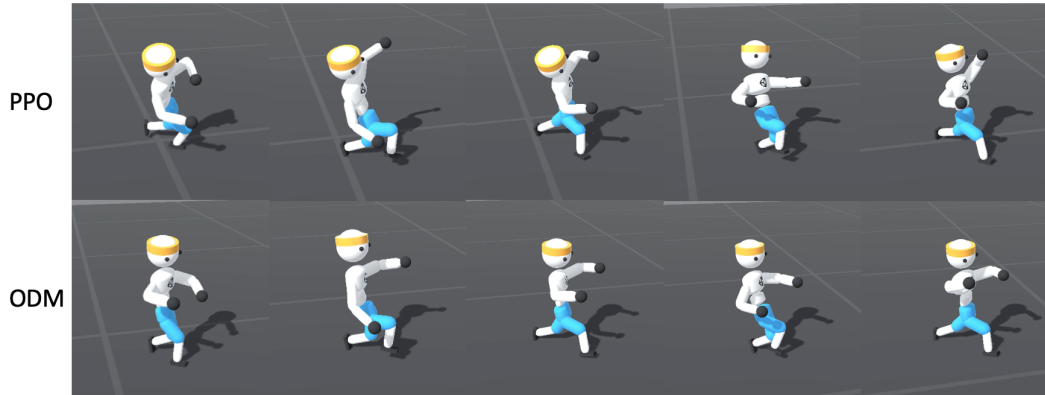


Figure 5: ODM improves motion fluency and coherence in the walker environment. Keyframes are screened on Second 1, 2, 3, 4, 5, respectively. The video can be found on the website.

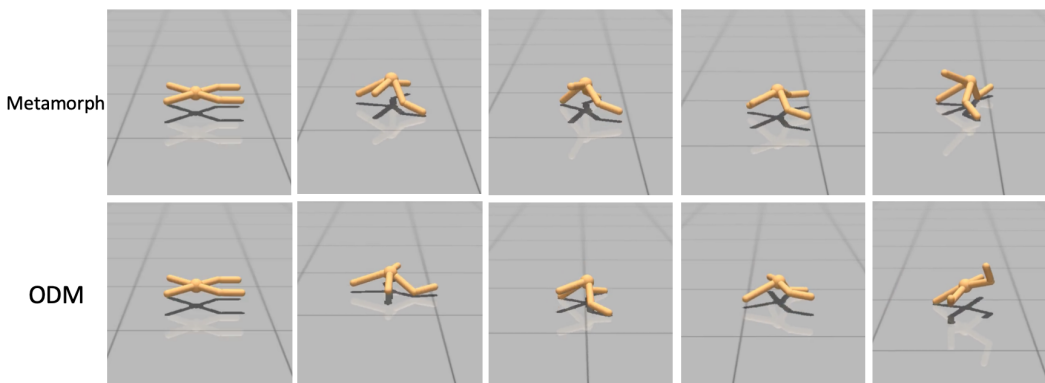


Figure 6: ODM improves motion agility with visualization of a typical unimal agent. Keyframes are screened evenly from the 30-second video.

some self-adaptive model structure (e.g. Hypernetwork Ha et al. [2017]) in these modules, it is possible to use one unified model to represent the generalist agent. Another potential improvement is to add the value/return prediction into the sequence modeled by the casual transformer. That is, the agent is able to estimate 'the value of its action' before the action is actually conducted, which is also known as 'metacognition' Conway-Smith and West [2022]. The last interesting topic is the potential training conflict when training switch from offline to online. That might be improved by some hyperparameter tuning (out of this paper's scope), e.g., some warmup schedule of L^{PPO} during finetuning; but could also be improved by better accommodation of the offline phase knowledge to the online phase. However, these are out of this paper's scope and would require further research and experimentation.

7 Conclusion

In this paper, we propose a learning framework to provide a universal body control policy for arbitrary body shapes, environments, and tasks. This work is motivated by the intelligence development process in the natural world, where the agent can learn from others, reinforce with their own experiences, and utilize the world knowledge. To achieve this, we propose a two-dimensional transformer structure that encodes both the state-action morphological information and the time-sequential decision-making process. This framework is designed to be trained in a two-phase training paradigm, where the agent first learns from offline demonstrations of experts on different skill levels and tasks, then interacts with its own environment and reinforces its own skill through on-policy reinforcement learning. By pretraining the demonstration datasets, ODM can quickly warm up and learn the necessary knowledge

to perform the desired task, while the target environment continues to reinforce the universal policy. The results of our study suggest that our methodology is able to achieve embodied control over a wide range of tasks and environments, enabling agents to perform complex tasks in real-world scenarios. The results of our study contribute to the study of general artificial intelligence in embodied and cognitive fields.

References

- Lili Chen, Kevin Lu, Aravind Rajeswaran, Kimin Lee, Aditya Grover, Misha Laskin, Pieter Abbeel, Aravind Srinivas, and Igor Mordatch. Decision transformer: Reinforcement learning via sequence modeling. In M. Ranzato, A. Beygelzimer, Y. Dauphin, P.S. Liang, and J. Wortman Vaughan, editors, *Advances in Neural Information Processing Systems*, volume 34, pages 15084–15097. Curran Associates, Inc., 2021. URL <https://proceedings.neurips.cc/paper/2021/file/7f489f642a0ddb10272b5c31057f0663-Paper.pdf>.
- Brendan Conway-Smith and Robert L. West. System-1 and system-2 realized within the common model of cognition. In *AAAI FALL SYMPOSIUM SERIES*, 2022.
- Justin Fu, Aviral Kumar, Ofir Nachum, George Tucker, and Sergey Levine. D4RL: datasets for deep data-driven reinforcement learning. *CoRR*, abs/2004.07219, 2020. URL <https://arxiv.org/abs/2004.07219>.
- Scott Fujimoto, David Meger, and Doina Precup. Off-policy deep reinforcement learning without exploration. In Kamalika Chaudhuri and Ruslan Salakhutdinov, editors, *Proceedings of the 36th International Conference on Machine Learning*, volume 97 of *Proceedings of Machine Learning Research*, pages 2052–2062. PMLR, 09–15 Jun 2019. URL <https://proceedings.mlr.press/v97/fujimoto19a.html>.
- Agrim Gupta, Silvio Savarese, Surya Ganguli, and Li Fei-Fei. Embodied intelligence via learning and evolution. *Nature Communications*, 12, 2021. URL <https://doi.org/10.1038/s41467-021-25874-z>.
- Agrim Gupta, Linxi Fan, Surya Ganguli, and Li Fei-Fei. Metamorph: Learning universal controllers with transformers. In *The Tenth International Conference on Learning Representations (ICLR)*, 2022.
- David Ha and Jürgen Schmidhuber. Recurrent world models facilitate policy evolution. In S. Bengio, H. Wallach, H. Larochelle, K. Grauman, N. Cesa-Bianchi, and R. Garnett, editors, *Advances in Neural Information Processing Systems*, volume 31. Curran Associates, Inc., 2018. URL <https://proceedings.neurips.cc/paper/2018/file/2de5d16682c3c35007e4e92982f1a2ba-Paper.pdf>.
- David Ha, Andrew Dai, and Quoc V. Le. Hypernetworks. In *International Conference on Learning Representations*, 2017. URL <https://openreview.net/pdf?id=rkpACe1lx>.
- Matej Hoffmann and Rolf Pfeifer. The implications of embodiment for behavior and cognition: animal and robotic case studies. *CoRR*, abs/1202.0440, 2012. URL <http://arxiv.org/abs/1202.0440>.
- Wenlong Huang, Igor Mordatch, and Deepak Pathak. One policy to control them all: Shared modular policies for agent-agnostic control. In *ICML*, 2020.
- Michael Janner, Qiyang Li, and Sergey Levine. Offline reinforcement learning as one big sequence modeling problem. In M. Ranzato, A. Beygelzimer, Y. Dauphin, P.S. Liang, and J. Wortman Vaughan, editors, *Advances in Neural Information Processing Systems*, volume 34, pages 1273–1286. Curran Associates, Inc., 2021. URL <https://proceedings.neurips.cc/paper/2021/file/099fe6b0b444c23836c4a5d07346082b-Paper.pdf>.
- Arthur Juliani, Vincent-Pierre Berges, Esh Vckay, Yuan Gao, Hunter Henry, Marwan Mattar, and Danny Lange. Unity: A general platform for intelligent agents. *CoRR*, abs/1809.02627, 2018. URL <http://arxiv.org/abs/1809.02627>.

- Ilya Kostrikov, Ashvin Nair, and Sergey Levine. Offline reinforcement learning with implicit q-learning. 2021.
- Aviral Kumar, Aurick Zhou, George Tucker, and Sergey Levine. Conservative q-learning for offline reinforcement learning. In H. Larochelle, M. Ranzato, R. Hadsell, M.F. Balcan, and H. Lin, editors, *Advances in Neural Information Processing Systems*, volume 33, pages 1179–1191. Curran Associates, Inc., 2020. URL <https://proceedings.neurips.cc/paper/2020/file/0d2b2061826a5df3221116a5085a6052-Paper.pdf>.
- Vitaly Kurin, Maximilian Igl, Tim Rocktäschel, Wendelin Boehmer, and Shimon Whiteson. My body is a cage: the role of morphology in graph-based incompatible control. In *International Conference on Learning Representations*, 2021. URL <https://openreview.net/forum?id=N3zUDGN510>.
- Kuang-Huei Lee, Vincent-Pierre Berges, Esh Vekay, Yuan Gao, Hunter Henry, Marwan Mattar, and Danny Lange. Multi-game decision transformers. *Arxiv*, abs/2205.15241v1, 2022. URL <https://arxiv.org/abs/2205.15241v1>.
- Volodymyr Mnih, Koray Kavukcuoglu, David Silver, Andrei A. Rusu, Joel Veness, Marc G. Bellemare, Alex Graves, Martin Riedmiller, Andreas K. Fidjeland, Georg Ostrovski, Stig Petersen, Charles Beattie, Amir Sadik, Ioannis Antonoglou, Helen King, Dharshan Kumaran, Daan Wierstra, Shane Legg, and Demis Hassabis. Human-level control through deep reinforcement learning. *Nature*, 518(7540):529–533, February 2015. ISSN 00280836. URL <http://dx.doi.org/10.1038/nature14236>.
- Scott Reed, Konrad Zolna, Emilio Parisotto, Sergio Gomez Colmenarejo, Gabriel Barth-Maron Alexander Novikov, Mai Gimenez, Yury Sulsky, Jackie Kay, Jost Tobias Springenberg, Tom Eccles, Jake Bruce, Ali Razavi, Ashley Edwards, Nicolas Heess, Yutian Chen, Raia Hadsell, Oriol Vinyals, Mahyar Bordbar, and Nando de Freitas. A generalist agent. *Transactions on Machine Learning Research*, 11, 2022.
- John Schulman, Philipp Moritz, Sergey Levine, Michael I. Jordan, and Pieter Abbeel. High-dimensional continuous control using generalized advantage estimation. In Yoshua Bengio and Yann LeCun, editors, *4th International Conference on Learning Representations, ICLR 2016, San Juan, Puerto Rico, May 2-4, 2016, Conference Track Proceedings*, 2016. URL <http://arxiv.org/abs/1506.02438>.
- John Schulman, Filip Wolski, Prafulla Dhariwal, Alec Radford, and Oleg Klimov. Proximal policy optimization algorithms. *CoRR*, abs/1707.06347, 2017. URL <http://arxiv.org/abs/1707.06347>.
- Ashish Vaswani, Noam Shazeer, Niki Parmar, Jakob Uszkoreit, Llion Jones, Aidan N. Gomez, Lukasz Kaiser, and Illia Polosukhin. Attention is all you need. In *Proceedings of the 30th International Conference on Neural Information Processing Systems, NIPS '17*, 2017.
- Philipp Wu, Alejandro Escontrela, Danijar Hafner, Pieter Abbeel, and Ken Goldberg. Daydreamer: World models for physical robot learning. In *CoRL*, 2022.
- Mengdi Xu, Yikang Shen, Shun Zhang, Yuchen Lu, Ding Zhao, Joshua Tenenbaum, and Chuang Gan. Prompting decision transformer for few-shot policy generalization. In Kamalika Chaudhuri, Stefanie Jegelka, Le Song, Csaba Szepesvari, Gang Niu, and Sivan Sabato, editors, *Proceedings of the 39th International Conference on Machine Learning*, volume 162 of *Proceedings of Machine Learning Research*, pages 24631–24645. PMLR, 17–23 Jul 2022. URL <https://proceedings.mlr.press/v162/xu22g.html>.
- Qinqing Zheng, Amy Zhang, and Aditya Grover. Online decision transformer. In Kamalika Chaudhuri, Stefanie Jegelka, Le Song, Csaba Szepesvari, Gang Niu, and Sivan Sabato, editors, *Proceedings of the 39th International Conference on Machine Learning*, volume 162 of *Proceedings of Machine Learning Research*, pages 27042–27059. PMLR, 17–23 Jul 2022. URL <https://proceedings.mlr.press/v162/zheng22c.html>.

A Additional Methodology Details

During the RL study, the agent generate its action from its policy $\pi(a_t|s_t)$ and push the environment stage forward. This interactive process yields the following episode sequence:

$$\tau_{0:T} = \{s_0, a_0, r_0, s_1, a_1, r_1, \dots, s_T, a_T, r_T\} \quad (17)$$

in which T means the episode ends or reaching the maximum time length. RL then solves the sequential decision making problem by finding π such that $\max_{\pi} \mathbb{E}_{\tau \sim \pi}(R)$ in which the episode return defined as

$$R := \sum_{t=0}^T \gamma^t r_t \quad (18)$$

with $\gamma \in [0, 1)$ as the discounted factor.

The classical PPO methodology inherits from the famous actor-critic framework. The critic generates the state value estimate $V(s)$, with its loss calculated from Bellman function by bootstrapping the state value function

$$L^{\text{Critic}} = \mathbb{E}_{s \sim d^{\pi}} [(r_t + \gamma(V_{\theta_{\text{old}}}(s_{t+1}) - V_{\theta}(s_t)))^2]$$

On the other hand, generalized advantage estimation (GAE) [Schulman et al., 2016] is employed to help calculate the action advantage A_t by traversing the episode backward

$$\hat{A}_t = \delta_t + (\gamma\lambda)\delta_{t+1} + \dots + (\gamma\lambda)^{T-t+1}\delta_{T-1} \quad (19)$$

$$\delta_t = r_t + \gamma V(s_{t+1}) - V(s_t) \quad (20)$$

then the actor is learned by maximizing the surrogate objective of A_t according to the policy-gradient theorem

$$L^{\text{Actor}} = \text{CLIP}\left(\mathbb{E}_t \frac{\pi_{\theta_{\text{old}}}(a_t|s_t)}{\pi_{\theta}(a_t|s_t)} \hat{A}_t - \beta \text{KL}[\pi_{\theta_{\text{old}}}(\cdot|s_t), \pi_{\theta}(\cdot|s_t)]\right) \quad (21)$$

in which the CLIP function means clipping the object by $[1 - \epsilon, 1 + \epsilon]\hat{A}_t$, and KL denotes the famous K-L divergence.

A PPO policy update is then conducted by minimizing the objective upon each iteration:

$$L^{\text{PPO}} = -\eta_A L^{\text{Actor}} + \eta_C L^{\text{Critic}}$$

B Additional Implementation Details

For practical consideration, input and output sequences are truncated by a window length T_w , with padding time mask for episodes shorter than T_w . The timestep embedding is also considered and concatenated into the latent variable.

To emphasize the instant impact, we further conduct a multi-head attention by querying the target variable and marking the input variable as key and value:

$$\begin{aligned} \hat{a}_t^p &\leftarrow \hat{a}_t^p + \text{Attention}(\text{Q}=\hat{a}_t^p, \text{K}=s_t^p, \text{V}=s_t^p) \\ \hat{s}_t^p &\leftarrow \hat{s}_t^p + \text{Attention}(\text{Q}=\hat{s}_t^p, \text{K}=a_{t-1}^p, \text{V}=a_{t-1}^p) \end{aligned} \quad (22)$$

Table 8 lists most hyper-parameters in our implementation.

Table 8: Hyper-parameters

Parameter	Value
γ	0.90
ϵ	0.1
β	0.1
λ	0.1
N	32
T	1000
T_w	10
e	128
η_A	-1.0
η_C	0.1
η_p	0.1
η_i	1.0
η_1	1.0
η_2	0.00001
# attention head	2
attention dimension	1024
layers(Embed _o)	$[n, e]$
layers(Embed _x)	$[x, e]$
layers(Embed _a)	$[m, e]$
layers(Embed _s)	$[(K + 1)e, e]$
layers(Proj _s)	$[e, n_s]$
layers(Proj _a)	$[e, n_a]$
layers(Proj _v)	$[e, 1]$
learning rate (pretraining)	0.00001
learning rate (finetuning)	0.0005